

## MODULATION OF WEAK MOTION SITE TRANSFER FUNCTIONS BY NON-LINEAR BEHAVIOR: A STATISTICAL COMPARISON OF 1D NUMERICAL SIMULATION WITH KIKNET DATA.

Michelle Almakari<sup>1</sup>, Julie Régnier<sup>2</sup>, Christelle Salameh<sup>3</sup>, Héloïse Cadet<sup>4</sup>, Pierre-Yves Bard<sup>5</sup>,  
Fernando Lopez-Caballero<sup>6</sup> and Cécile Cornou<sup>5</sup>

<sup>1</sup>Master Student, ISTerre, Université Grenoble Alpes / IFSTTAR / IRD / CNRS, Grenoble, France

<sup>2</sup>Scientist, CEREMA, DTer Méditerranée, Nice, France

<sup>3</sup>PhD Student, ISTerre, Université Grenoble Alpes / IFSTTAR / IRD / CNRS, Grenoble, France

<sup>4</sup>Research engineer, ADRGT, Grenoble, France

<sup>5</sup>Scientist, ISTerre, Université Grenoble Alpes / IFSTTAR / IRD / CNRS, Grenoble, France

<sup>6</sup>Associate Professor, Ecole Centrale de Paris, Chatenay-Malabry, France

Email: [michelle\\_makari@hotmail.com](mailto:michelle_makari@hotmail.com), [julie.regnier@cerema.fr](mailto:julie.regnier@cerema.fr), [christelle.salameh@univ-grenoble-alpes.fr](mailto:christelle.salameh@univ-grenoble-alpes.fr),  
[h.cadet@adrgt.org](mailto:h.cadet@adrgt.org), [pierre-yves.bard@univ-grenoble-alpes.fr](mailto:pierre-yves.bard@univ-grenoble-alpes.fr), [fernando.lopez-caballero@centralesupelec.fr](mailto:fernando.lopez-caballero@centralesupelec.fr),  
[cecile.cornou@univ-grenoble-alpes.fr](mailto:cecile.cornou@univ-grenoble-alpes.fr)

### ABSTRACT

The non-linear behavior in soft to moderately stiff soils modifies the linear site response, generally by shifting the resonance frequencies towards lower values, and reducing the high-frequency motion in relation to shear modulus decrease and damping increase with increasing loading. The resulting “modulation” of the site response may be quantified by the nonlinear to linear site response ratio,  $RSR_{NL-L}$ , comparing the Fourier transfer function for strong events and for weak events. As shown by Régnier et al., 2016 who performed such an analysis for 174 sites of the Japanese KiK-net network, and 3 "strong motion thresholds" [surface PGA  $\geq 1, 2$  and  $3 \text{ m/s}^2$ ], this ratio exhibits a "typical shape"; with a low frequency part above 1 and a high frequency part generally below 1, separated by a transition zone around a site-dependent frequency labelled  $f_{NL}$  (characterized by  $RSR_{NL-L} = 1$ ). The present work intends to compare these observations with the results of extensive non-linear numerical simulation, using about 820 different shear wave velocity profiles from real sites, and non-linear characteristics adapted from the EPRI and Imperial Valley models for cohesionless and cohesive soils, respectively. The response of each soil column to 60 realistic input motion with PGA in the range from  $0.01$  to  $4 \text{ m/s}^2$  was computed with the NOAH code developed by F. Bonilla. The analysis was performed in the same way as in Régnier et al., 2016, using different surface PGA ranges to classify the results:  $[1, 2 \text{ m/s}^2]$ ,  $[2, 3 \text{ m/s}^2]$ ,  $[3, 4 \text{ m/s}^2]$ ,  $[4, 5 \text{ m/s}^2]$ ,  $[5, 6 \text{ m/s}^2]$ , and  $[6, 7 \text{ m/s}^2]$ . Non-linear soil behavior results in significant site response modifications even for moderate PGA values of  $100 \text{ cm/s}^2$ , in that case mainly for soft soils with low  $V_{S30}$  value. The resulting  $RSR_{NL-L}$  functions exhibit a qualitatively similar shape compared to instrumental data.  $f_{NL}$  values exhibit a satisfactory correlation with site classifications based on either  $V_{S30}$  or  $f_0$ : the lower  $V_{S30}$  or  $f_0$ , the lower  $f_{NL}$ . It is also found that for high-frequency or stiff sites, the ratio  $f_{NL}/f_0$  is very close to 1, while it exhibits a large scatter for low frequency sites, with values in the range  $[1, 10]$ , indicating the concentration of non-linearities in relatively shallow layers. The amount of low-frequency amplification (i.e., for  $f < f_{NL}$ ) increases with increasing non-linearity, i.e., with increasing PGA and/or strain, and the same for the high-frequency (i.e.,  $f > f_{NL}$ ) reduction. However, from a quantitative viewpoint, the present numerical simulations seem to overestimate the non-linearity for deep sites with low fundamental frequency. The final aim to propose a model allowing to apply a frequency-dependent “NL modulation” to the measured or computed linear transfer functions, as a function of PGA level and site characteristics, including  $V_{S30}$  and  $f_0$ , therefore requires further investigations on the actual behavior of such deep deposits.

Keywords: *non-linear behavior, KiK-Net, numerical simulation, site classification*

## INTRODUCTION

Lithological site effects have long been recognized as significantly impacting the surface ground motion. Besides resonance and geometrical effects, the non-linear behavior of soft soils is one important component that should be taken into consideration in determining the site response. The early works of Seed and Idriss (1969) and Hardin and Drnevich (1972a, 1972b), convinced the geotechnical engineering community that soft soils exhibit strong nonlinearities during earthquakes, with an onset of degradation of soil mechanical properties starting as very low strain levels. As outlined for instance in Erdik (1987) or Finn (1991), the high levels of shear strains generated in soft (low velocity) soils by strong shaking draw them into highly hysteretic stress strain loops and induce a significantly, or even completely modified site response. The deficiency of direct evidence in early (and scarce) strong motion observations ([Aki & Richards, 1980](#)) together with an over-prediction of non-linear effects in the 1985 Michoacan, Mexico and the 1989 Loma Prieta, California, earthquakes by the early degradation curves, led some delay (1-2 decades) for the seismological community to endorse the importance of such non-linear effects. Nonetheless the multiplication of accelerometric stations in the recent decades provided numerous strong motion recordings especially in vertical arrays, which now present very solid evidence of significant NL effects, with reduction of amplification and shift of resonant frequencies under strong loading ([Beresnev & Wen, 1996](#)). It is therefore highly important to try and quantify the impact of this non-linear behavior on the site response. This may be done either on a site-specific basis, with detailed information on the soil characteristics (velocity profile, non-linear properties), or on a more statistical basis, trying to estimate the average effects for different classes of soil, as implemented in recent GMPEs, see for instance [Choi and Stewart \(2005\)](#), [Walling et al. \(2008\)](#), [Sandikkaya et al. \(2013\)](#), and [Kamai et al. \(2014\)](#). The present work lies in the latter category, with a long-term objective to propose stand-alone "SAPes" (Site Amplification Prediction Equations) taking into account NL effects in a new way and in the Fourier domain instead of the response spectra domain

Typically, the main, first order, effects of non-linearity may be summarized as follows for the simple example of a homogeneous layer lying on a half-space. The decrease of the shear modulus  $G$  with increasing strain will result in a decrease of the shear wave velocity  $V_s = \sqrt{G/\rho}$ , where  $\rho$  is the mass density, which in turn will result in a decrease of the fundamental frequency  $f_0 = V_s/4H$ . On the other hand, the hysteresis loops induce a larger and larger damping as strain increases, which in turn results in a reduction of the corresponding amplification as damping effects override effects of increased impedance contrast ( $A_0 = C / (1 + 0.5 \pi \zeta C)$ , where  $C$  is the mechanical impedance contrast between the underlying bedrock and the soft layer). Of course, this example is oversimplified with respect to the real Earth, presenting at least multi-layered soil columns, very often water saturated beyond some depth. However, it is fully consistent with the empirical evidences and observations for non-linear soil behavior reported in the literature, which are: first, an increase in the site response amplitude at relatively low frequencies, because of the frequency shift ([Frankel et al., 2002](#); [Régnier et al., 2013](#)); second, a de-amplification in the high frequency for sites that do not exhibit pore pressure effects ([Bonilla et al., 2005](#); [Frankel et al., 2002](#); [Roten et al., 2013](#)).

It therefore allows the concept of the nonlinear to linear site response ratio,  $RSR_{NL-L}$ , first proposed by [Régnier et al \(2013\)](#) to investigate the modulation of weak motion, linear site response by non-linear soil behavior. As expected from the simple 1-layer over half-space case, this ratio exhibits a "typical shape", with a low frequency part above 1 and a high frequency part generally below 1, separated by a transition zone around a site-dependent frequency labelled  $f_{NL}$ , characterized by a unit value of the  $RSR_{NL-L}$  ratio. The present work intends to confront the outcomes of a comprehensive set of numerical simulations with the actual observations presented by [Régnier et al. \(2016\)](#) from the analysis of a large set of KiK-net data and sites. The next paragraphs will present successively the set of numerical simulations (soil profiles, input accelerograms, non-linear parameters and computation code), an outline of the corresponding results and some indications of the comparison with actual observations.

## COMPUTATIONAL SET AND CALCULATION METHOD

### Soil Profiles

For this work, a set of 820 multilayered soil profiles corresponding to real sites was considered. It was originally compiled by C. Cornou and consists of 593 Japanese KiK-net sites, 205 sites from the US and made available by D. Boore ([http://www.daveboore.com/data\\_online.html](http://www.daveboore.com/data_online.html)), and 22 European sites measured during the NERIES project (Bard et al., 2010). The KiKnet velocity profiles were directly collected at <http://www.kyoshin.bosai.go.jp>, and consist of surface-to-downhole measurements of S- and P-wave velocities. Some of these profiles were modified as explained in Salameh (2016) in order to have a minimum velocity of 800 m/s in the underlying half-space (= bedrock). The main characteristics of the set of resulting profiles are summarized in Figure 1 with the distribution of  $V_{S30}$  (m/s),  $f_0$  (Hz), thickness (m), and bedrock shear wave velocity (m/s). This set is thus mainly consisting of usual to stiff soils, with shallow to intermediate thickness (smaller than 200 m in most cases, with only few sites with fundamental frequency below 1 Hz), and "normally hard" to very hard bedrock.

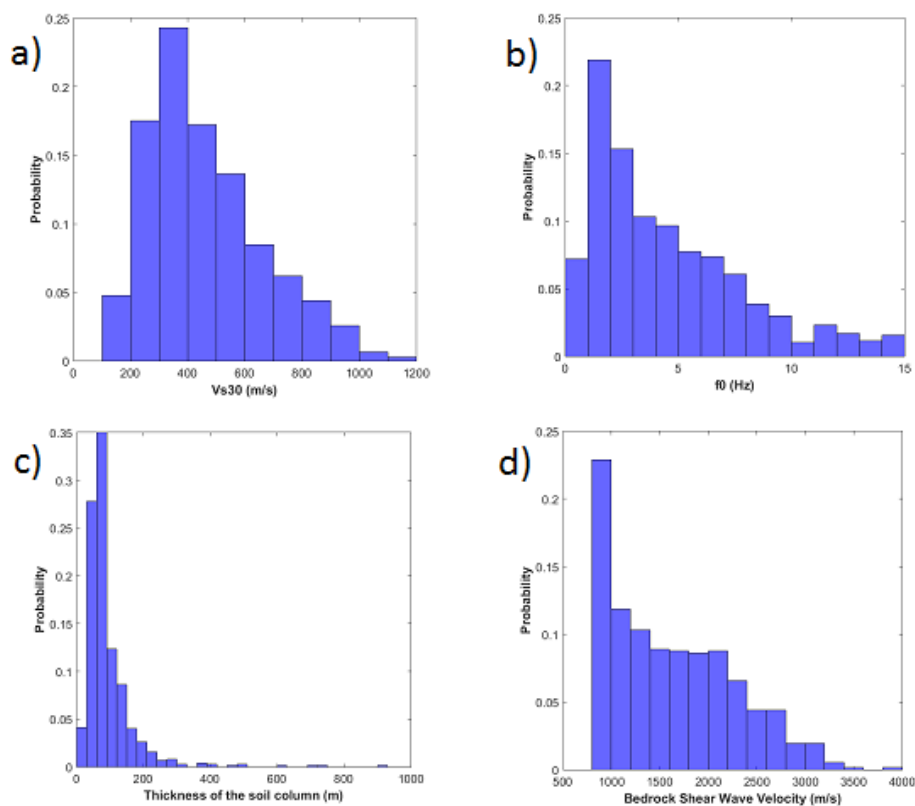


Figure 1. Overview of main site characteristics for the considered soil profiles : Distribution of a)  $V_{S30}$  values, b)  $f_0$  values, c) total thickness values and d) bedrock shear wave velocity.

### Seismic Loading

As this work was part of a more comprehensive endeavour on damage increase linked with site response (Salameh, 2016; Salameh et al., 2016), it was decided for simplicity purposes to use a set of synthetic input accelerograms. A set of 60 time histories was generated using the approach proposed by Sabetta and Pugliese (1996), which allow to obtain realistic waveforms presenting both frequency and non-stationary characteristics representative of real accelerograms. They correspond to scenario earthquakes with a magnitude range from 3 to 7, recorded at distances from 2 to 100 km, and PGA peak ground acceleration (PGA) ranging between  $0.02 \text{ m/s}^2$  and  $4.2 \text{ m/s}^2$ . Such synthetics exhibit average characteristics and relatively smooth spectra : a test was therefore performed for a few sites to

investigate the sensitivity of the non-linear modulation of site response to the details of input accelerograms by replacing, for a small number of representative sites, the set of 60 synthetic accelerograms by a set of 60 real waveforms covering the same magnitude, distance and PGA ranges. The overall results remain unchanged, despite some slight changes in the response to individual waveforms.

### Non-Linear Models

Only velocity profiles are available for the 820 sites considered, without any indication on their non-linear parameters. It was thus necessary to make arbitrary decisions on the way to assign non-linear characteristics to each layer of each velocity profile. As a first step, simple attempt, we followed the procedure proposed in [Kamai et al. \(2014\)](#), who use two sets of "generic", depth dependent NL degradation curves (see Figure 2) depending on the soil cohesion: the EPRI curves are assigned to cohesionless soils, while "IV" (Imperial valley) curves are assigned to cohesive soils. The PEER study mentioned above decided that all soil profiles having a  $V_{s30}$  value lower than 190 m/s would be considered as cohesive ("IV") from the surface down to the bedrock, while sites with  $V_{s30}$  higher than 190 m/s should be considered as cohesionless again from the surface down to the bedrock. Although this assignment procedure is very crude, we think it provides a first set of results that is worth being analyzed in a statistical sense, which is the only purpose of the present work.

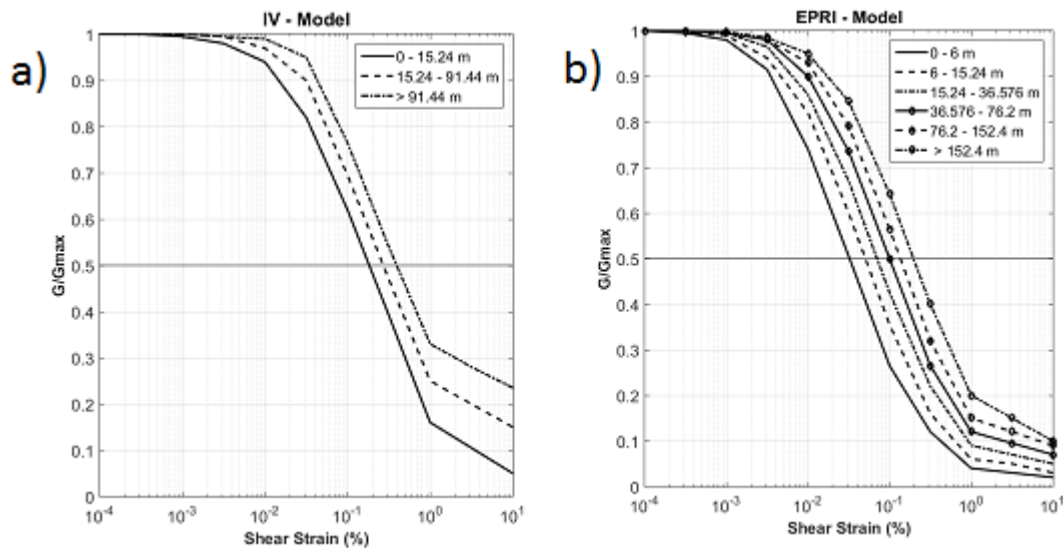


Figure 2. Degradation Curves: a) IV Model; b) EPRI Model.

### Non-Linear Code

In this work, the non-linear wave propagation is computed using the NOAH code (Bonilla L. , 2001). This NONlinear Anelastic Hysteretic finite difference code computes the nonlinear site response for vertically incident plane SH waves, using the strain space multi-shear mechanism model developed by (Towhata & Ishihara, 1985) and [Iai et al. \(1990\)](#). For this preliminary study, we decided to start with the simplest possible case, i.e. without considering the pore pressure effects: all the present computations were performed following a total stress analysis. In the code implementation that we used, the non-linear soil properties are not specified through the degradation curves but through the strength of the soil, characterized by its cohesion and friction angles. The EPRI and IV curves were thus converted into depth-dependent friction angles, with cohesion values assumed to be 0 for cohesion-less soils, and 30 kPa for cohesive soils. The so obtained friction angles were found in some cases to have unrealistic (very low or very high) values, and were then bounded by the limiting values of  $25^\circ$  and  $45^\circ$ .

## OVERVIEW OF NON-LINEAR EFFECTS

### Time domain : saturation of the surface PGA

Under seismic loading, when the shear strain increases, the soil profile goes farther and farther into the non-linear domain especially in the weakest layer, the corresponding shear stress is getting nearer and nearer to its asymptotic value  $\tau_{\max}$ , and cannot transmit accelerations higher than (approximately)  $\tau_{\max} / \rho \cdot z$ , where  $\rho$  is the unit mass and  $z$  the depth of the considered layer. As a consequence, at each site, the peak surface acceleration cannot exceed the threshold value corresponding to its weakest layer where the higher strains are developed. This "saturation" value of pga appears very clearly in Figure 3 displaying the variation of surface pga with peak strain for the whole set of 820 sites and 60 input accelerograms. For a given site, low input pga values generate small peak strain within the soil profile, which remains well below the corresponding "reference strain"  $\gamma_{\text{ref}} = \tau_{\max} / G_{\text{max}}$  (where  $G_{\text{max}}$  is the low strain shear modulus at the depth of the peak strain). When the input pga increases, the peak strain  $\gamma_{\text{max}}$  keeps increasing, and when it gets comparable to or higher than  $\gamma_{\text{ref}}$ , the soil goes far into the non-linear domain, and the transmitted acceleration gets close to its saturation value. This explains the asymptotic shape of curves in Figure 3, which also indicates that the saturation pga is decreasing with decreasing soil stiffness : the lowest saturation pga (around 2 m/s<sup>2</sup>) correspond to red points, i.e. those with  $V_{S30} < 180$  m/s, while the largest (around 7 m/s<sup>2</sup>) correspond to magenta points i.e. with  $V_{S30} > 760$  m/s.

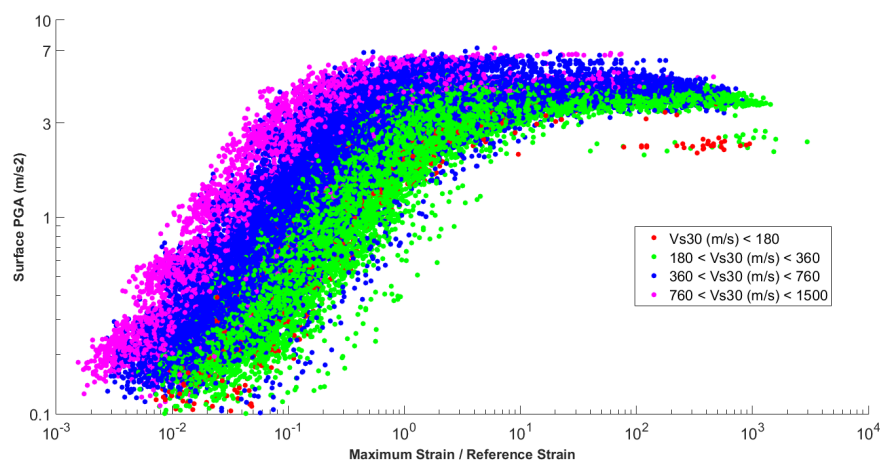


Figure 3. Saturation of the surface PGA for different  $V_{S30}$  site classes. One point in this graph represents the surface pga as a function of peak "relative strain" (ratio  $\gamma_{\text{max}}/\gamma_{\text{ref}}$  where  $\gamma_{\text{max}}$  is the peak strain value along the whole profile and  $\gamma_{\text{ref}}$  is the reference strain at the corresponding depth). This plot gathers 49200 points corresponding to 820 sites and 60 input accelerograms, the different colors stand for different  $V_{S30}$  ranges.

In order to better capture the relation between saturation PGA and the characteristics of velocity profiles, we have plotted in Figure 4 the distribution of the  $f_0$  (left) and  $V_{S30}$  (right) values for the different ranges of saturation pga, from [2-3 m/s<sup>2</sup>] to over 7 m/s<sup>2</sup>. It appears very clearly that saturation pga increases a) with increasing  $f_0$ , and b) with increasing  $V_{S30}$  (two site parameters which are indeed only weakly correlated for the whole set of 820 sites we considered, see Salameh, 2016). In other terms, as expected, transmittable acceleration is the highest for stiff, shallow sites, while it is the smallest for deep, soft sites. This information can also be derived from Tables 1 and 2, which list the number of sites reaching a given surface PGA range (left column) in various site classes ( $f_0$  classes in Table 1,  $V_{S30}$  classes in Table 2). Deep soft soils, with  $V_{S30} < 180$  m/s or  $f_0 < 1$  Hz, exhibit a small value of saturation PGA, which never exceeds 4 m/s<sup>2</sup> regardless of the seismic outcrop excitation. One may also notice a slightly better correlation of saturation pga with  $V_{S30}$  compared to  $f_0$ .

Table 1 : Number of sites involved in various  $f_0$  classes for several surface PGA ranges

Surface PGA range (m/s <sup>2</sup> )	$f_0$ range (Hz)								Total	
	0.1 - 1		1 - 3.1		3.1 - 9.7		> 9.7			
1 - 2	56		297		355		63		771	
2 - 3	52	(93%)	291	(98%)	350	(98.5%)	63	(100%)	756	(98%)
3 - 4	19	(34%)	186	(63%)	322	(91%)	63	(100%)	590	(77%)
4 - 5	1	(2%)	35	(12%)	90	(25%)	35	(56%)	161	(21%)
5 - 6	-	(0%)	15	(5%)	44	(12%)	14	(22%)	73	(9.5%)
6 - 7	-	(0%)	-	(0%)	1	(0,3%)	1	(1,6%)	2	(0,3%)

Table 2 : Number of sites involved in various  $V_{S30}$  classes for several surface PGA ranges

Surface PGA range (m/s <sup>2</sup> )	$V_{S30}$ range (m/s)								Total	
	< 180		180 - 360		360 - 760		760 - 1500			
1 - 2	22		256		419		74		771	
2 - 3	19	(86%)	252	(98%)	411	(98.5%)	74	(100%)	756	(98%)
3 - 4	-	(0%)	135	(53%)	381	(91%)	74	(100%)	590	(77%)
4 - 5	-	(0%)	4	(1.6%)	107	(26%)	50	(68%)	161	(21%)
5 - 6	-	(0%)	-	(0%)	47	(11%)	26	(35%)	73	(9.5%)
6 - 7	-	(0%)	-	(0%)	1	(0,3%)	1	(1,6%)	2	(0,3%)

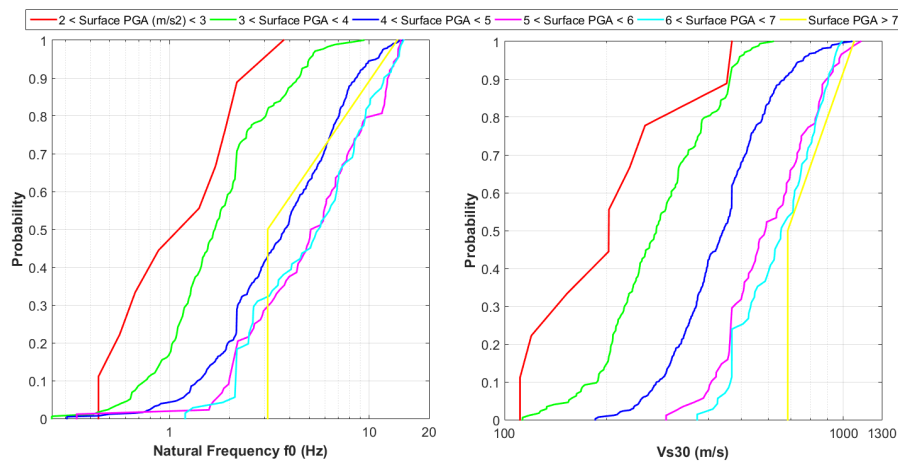


Figure 4. Cumulative Distribution Function of  $f_0$  (left) and  $V_{S30}$  (right) values for soil subsets grouped according to their saturation PGA.

### Frequency domain characterization of Non-Linear Site Response

The site response determines how each frequency in the bedrock (input) motion is amplified, or de-amplified by the soil deposit (Kramer, 1996). Thus, a site response may be viewed as a filter that acts upon some input signal to produce an output signal, in our case for vertically propagating SH waves. For the linear wave propagation case, the site transfer function (Fourier domain) is independent from the seismic excitation, with the first amplification peak (not necessarily the maximum one) occurring at the soil fundamental frequency  $f_0$ . Therefore, if the site response of a soil is known, its response to any seismic excitation is known. This is no longer true in the non-linear domain, as frequencies are shifted, and amplification changes from one case to another, depending on the degree of non-linearity reached. The site response with respect to a reference rock is defined in Eq. 1:

$$SSR = \frac{FT(Acc_{Surface})}{FT(Acc_{Outcrop})} \quad (1)$$

Where,  $FT(Acc_{Surface})$  and  $FT(Acc_{Outcrop})$  are the Fourier Spectra of the acceleration time history at the site surface and at a nearby outcropping rock, respectively. Linear site response is estimated by considering only weak motions, i.e. corresponding to outcropping rock PGA values from 0.001 to 0.25  $m/s^2$ ; while non-linear site response was calculated using strong motions, associated to Surface PGA values greater than 100  $cm/s^2$ ; and these site responses were averaged by classes of Surface PGA, namely [2-3  $m/s^2$ ], [3-4  $m/s^2$ ], [4-5  $m/s^2$ ], [5-6  $m/s^2$ ], and [6-7  $m/s^2$ ]. Given the site-specific PGA saturation phenomenon, this average is not computed over the same number of input accelerograms for each PGA class for different sites.

Figure 5 shows an example for one particular soil profile, "AKTH05", a stiff site from the KIK-net database with  $V_{S30} = 830$  m/s and  $f_0 = 8.7$  Hz. In this figure, sixty different site responses, from sixty different seismic excitations, are plotted. For weak seismic incident excitations, the transfer function exhibits a very low variability and presents its first peak for the value of fundamental frequency. For stronger motions (i.e., non black curves), higher surface PGA correspond to higher strains and higher excursions in the non-linear domain, and larger and larger changes in the site response.

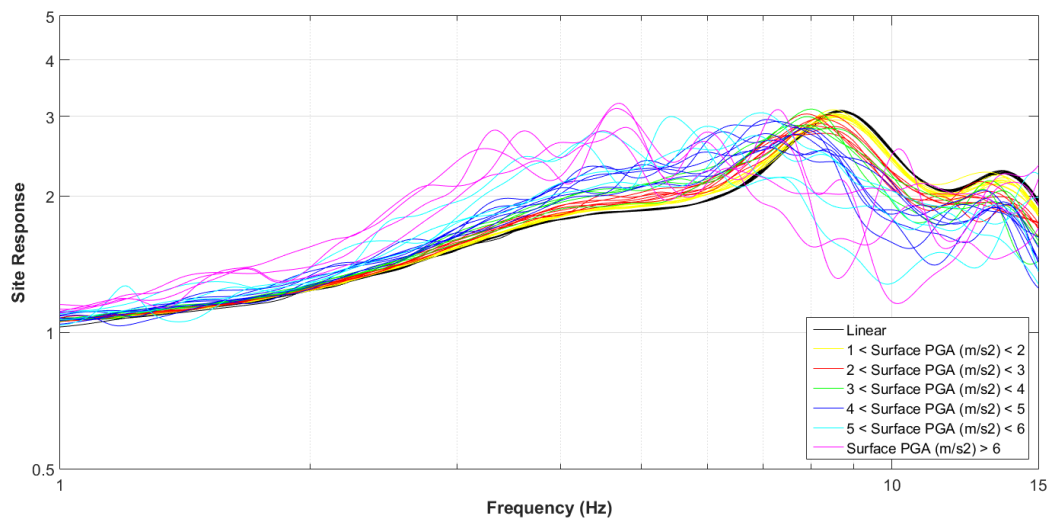


Figure 5. Simulated site Response (Surface to Outcropping rock SSR) for the KiKnet site "AKTH05" impinged by sixty different input accelerograms. The various colors correspond to various ranges for surface PGA

### ***Ratio of Site Response (Non-Linear to Linear)***

In order to analyze the effect of non-linear soil behavior on site response, we study the ratio of site response, non-linear to linear, denoted hereafter by  $RSR_{NL-L}$ . Accordingly, this ratio is calculated for each site by the logarithmic mean of the ratio between the geometrical average of non-linear response and the geometrical average of linear site responses,. The  $RSR_{NL-L}$  is therefore given for a site by Eq. 2:

$$\log_{10}(RSR_{NL-L}) = \frac{N_{weak}}{N_{strong}} \left[ \sum_{j=1}^{N_{strong}} \log_{10}(SSR_j) / \sum_{i=1}^{N_{weak}} \log_{10}(SSR_i) \right] \quad (2)$$

Where  $N_{strong}$  and  $N_{weak}$  are the number of accelerograms with a surface PGA falling in a given range larger than 100  $cm/s^2$ , and lower than 25  $cm/s^2$ , respectively; and  $j$  and  $i$  are the indexes on strong and weak motions, respectively. SSR is the site response with respect to a reference that is in our case outcropping rock. This ratio has been calculated for each site for all available ranges of surface PGA, namely [2-3  $m/s^2$ ], [3-4  $m/s^2$ ], [4-5  $m/s^2$ ], [5-6  $m/s^2$ ], and [6-7  $m/s^2$ ].

Figure 6 shows the ratio of simulated site response curves for the same (KiKnet) soil profile "AKTH05", with their corresponding standard deviation, and for each surface PGA range (the saturation PGA at this stiff site exceeds 6 m/s<sup>2</sup>). This curve exhibits a "typical shape" with a low frequency part above 1 and a high frequency part usually below 1, separated by a transition zone around a site-specific frequency labelled  $f_{NL}$ . From this plot, we can observe one more time, the effect of surface PGA. When it increases, the non-linear amplification and de-amplification increase, at low frequency and high frequency, respectively. As for the standard deviation, it is smaller at low frequency, while it increases at high frequency. Moreover, it increases with increasing Surface PGA, which is due to the non-linear behavior that is sensitive to the actual phase and frequency content of the input motion – in addition to its "level" approximated by the PGA proxy

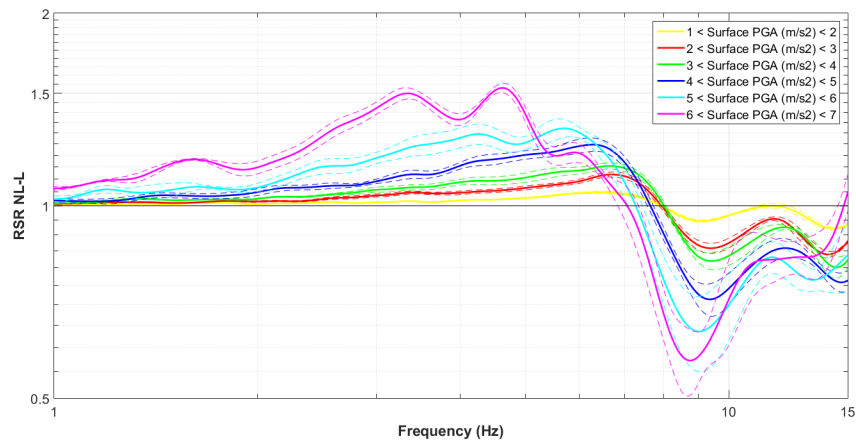


Figure 6. Ratio of simulated site response (Non-Linear - Linear) for the same AKTH05 site; solid lines represent the mean curve for each surface PGA class, while the dashed lines represent the mean curve  $\pm$  one standard deviation.

### *Selection of $f_{NL}$*

The expected shape of the site response ratio  $RSR_{NL-L}$  is presented in Figure 7, with an amplification and a de-amplification for frequencies lower and beyond a certain value called  $f_{NL}$ , respectively. The next step is to pick this frequency  $f_{NL}$  for each site from results and plots similar to Figure 6, and to investigate how it varies with different site parameters. For the site studied above, one may detect a slight reduction from one class of PGA to the next one, from 8 to 7 Hz, but nevertheless this reduction is very slight. The dependency of  $f_{NL}$  on PGA was systematically analyzed for the whole set of sites, and it was concluded that the PGA dependence was only marginal – at least for the NL parameters considered here -.

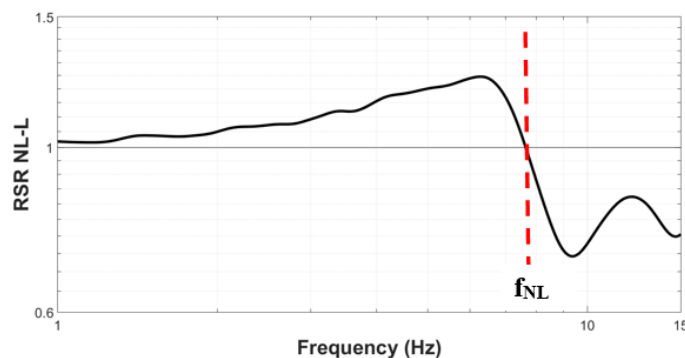


Figure 7. Typical shape of  $RSR_{NL-L}$  and selection of the site specific frequency  $f_{NL}$ .



## AVERAGE RESULTS FOR SITE CLASSES

One of the original objectives of this work is to propose a way to modify the linear site response by a "NL modulation", since linear site response is much easier both to measure and to predict than the NL response. In that aim, it is therefore interesting to investigate whether the "modulation functions", i.e., the  $RSR_{NL-L}$  curves, can be grouped according to the usual site classification schemes, in addition to the PGA level. Several site condition proxies have been proposed in the literature to classify the soils: the harmonic average shear wave velocity  $V_{S30}$  (by far the most widely used), the fundamental frequency  $f_0$ , the thickness down to a given velocity threshold ( $H_{800}$  for a 800 m/s threshold,  $Z_1$  or  $Z_{2.5}$  for the so-called "basin effects" and thresholds of 1 and 2.5 km/s, respectively), the velocity gradient B30, etc. ... This turned out to be a good approach to characterize either the linear site response (Cadet et al., 2012; Régnier et al., 2014), or the non-linear site response (Assimaki and Li, 2012; Bonilla et al., 2011; Régnier et al., 2013; Kamai et al., 2014). In the present work we investigated the first two classifications, i.e. those based on  $V_{S30}$  and  $f_0$ .

### $V_{S30}$ classification

We use the "classical" NEHRP (National Earthquake Hazard Reduction Program) classification to group sites according to their  $V_{S30}$  values, through the grouping intervals [100-180 m/s, NEHRP E], [180-360 m/s, NEHRP D], [360-760 m/s, NEHRP C] and [760-1500 m/s, NEHRP B]. For each site  $i$  belonging to a given site class  $cl$ , the average  $RSR_{NL-L,ia}$  was computed for a given surface PGA range  $a$ , and then a "class / PGA" average was derived as a geometrical average with equation (3)

$$\log_{10}(RSR_{NL-L,cl,a}) = \frac{1}{N_{cl,a}} \left[ \sum_{i=1}^{N_{cl,a}} \log_{10}(RSR_{NL-L,ia}) \right] \quad (3)$$

where  $N_{cl,a}$  is the number of sites in site class  $cl$  having surface pga in the considered range  $a$ . Thus, for each  $V_{S30}$  class and range of surface PGA, we have a single curve that represents the average non-linear modulation for sites in this group and for the corresponding surface pga. The corresponding results are displayed in Figure 8 with a comparison of the four  $V_{S30}$  classes for each of the 6 surface PGA ranges, from [1 – 2] m/s<sup>2</sup> to [6 – 7] m/s<sup>2</sup>. We can notice at first that the average non-linear frequency  $f_{NL}$  is almost independent of the surface pga range and increases with site stiffness:  $f_{NL}$  values are 0.7 Hz, 1.5 Hz, 5 Hz and 12 Hz, for the  $V_{S30}$  soil classes E to B, respectively. As a matter of fact, a stiff soil of NEHRP site category C or B, having a high  $V_{S30}$  value, can usually generate strong non-linearities only at shallow depth, and therefore its  $f_{NL}$  value is expected to be large. Moreover, we can see that the modulation amplitude is larger for soft sites than for stiff ones. For instance, considering the second class of surface PGA [2 – 3] m/s<sup>2</sup>, the values of the maximum low frequency amplification ( $f < f_{NL}$ ) are 1.18, 1.06, 1.04, 1.03, for the four  $V_{S30}$  classes, respectively.

Second, in order to investigate the effect of the PGA, we consider one particular  $V_{S30}$  class, and investigate how the modulation function  $RSR_{NL-L}$  evolves with the surface PGA range. Actually the low frequency ( $f < f_{NL}$ ) over-amplification increases, the high-frequency ( $f > f_{NL}$ ) de-amplification increases as well, while the switch between these two phenomena remains at the same frequency  $f_{NL}$ . For instance, taking the soft soils (i.e. NEHRP E  $V_{S30}$  lower than 180 m/s), the maximum low-frequency over- amplification increases from 1.09 to 1.19, for surface PGA range increasing [1 – 2] to [2 – 3] m/s<sup>2</sup>, while the corresponding maximum high-frequency de-amplification values goes from 0.75 to 0.55; meanwhile, as indicated before, the corresponding  $f_{NL}$  value of 0.7 Hz does not change. Finally, a last interesting result is that, for a given surface PGA range, the NL modulations are larger for soft sites, but as surface PGA increases, only stiffer and stiffer sites are concerned (saturation PGA is lower for softer sites), and the amplitude of the corresponding non-linear modulation increases and finally reaches higher values for stiff sites and high PGAs, than for soft soils and moderate surface PGAs.

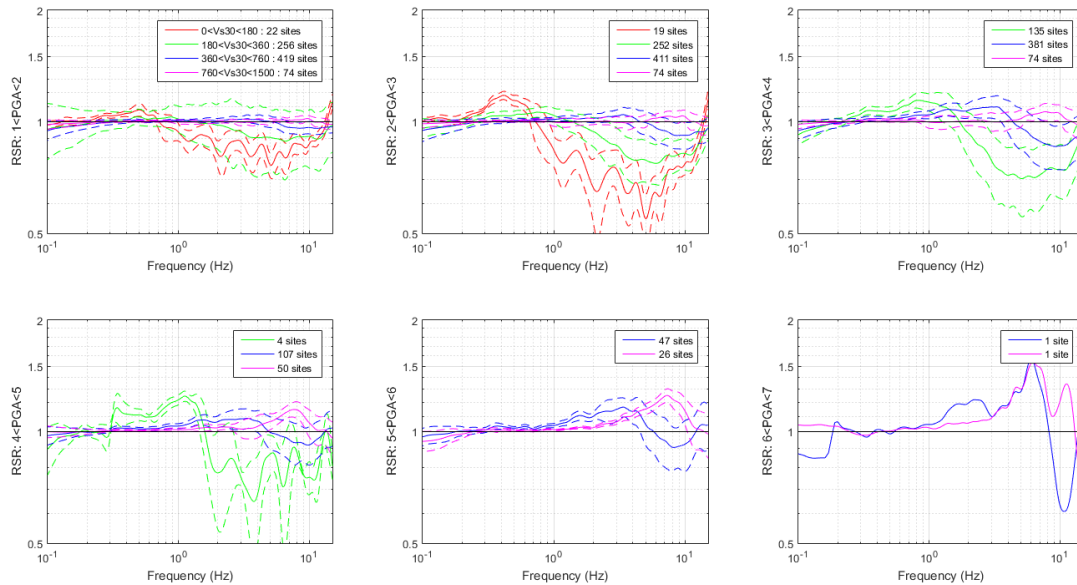


Figure 8. Average  $RSR_{NL-L}$  modulation functions for the different  $V_{S30}$  site classes (red: NEHRP E; green : NEHRP D; purple : NEHRP C; magenta : NEHRP B) for increasing surface PGA ranges (from left to right, and top to bottom). The number of sites for each set of (NEHRP class, surface pga range) is indicated in each frame.

### $f_0$ classification

The same analysis was done by classing the sites according to their fundamental frequency  $f_0$ . Four classes are considered :  $f_0 < 1$  Hz,  $[1, 3.1$  Hz],  $[3.1, 9.7$  Hz],  $[> 9.7$  Hz], the results of which are displayed on Figure 9. A similar behavior is observed: when the PGA increases, the non-linear modulation is accentuated;  $f_{NL}$  increases with increasing  $f_0$ .

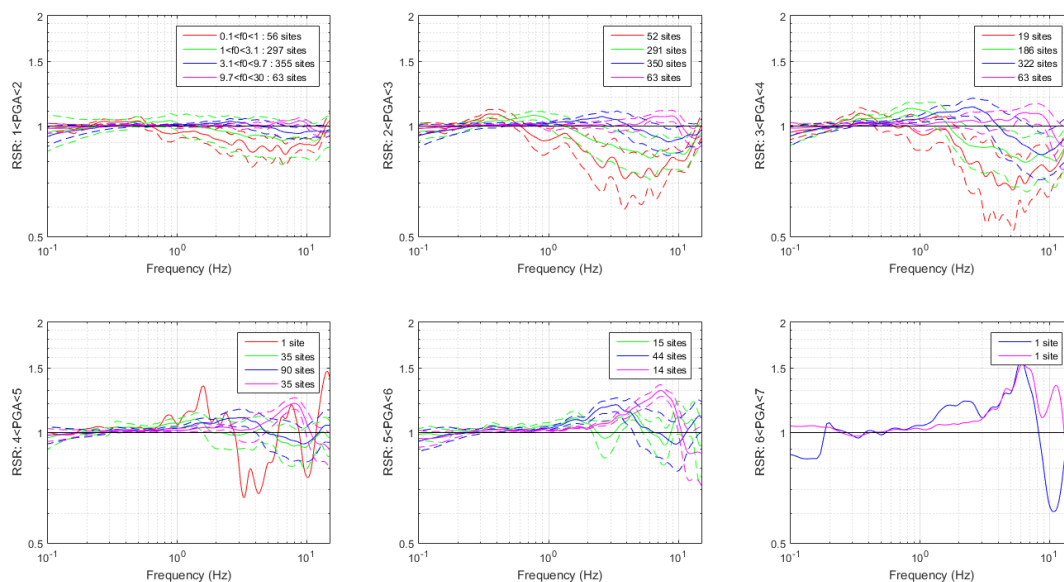


Figure 9. Average  $RSR_{NL-L}$  modulation functions for the different  $f_0$  site classes (red, green, purple and magenta for  $f_{NL} < 1$  Hz, 1-3.1 Hz, 3.1-9.7 Hz and  $> 9.7$  Hz, respectively) for increasing surface PGA ranges (from left to right, and top to bottom). The number of sites for each set of (NEHRP class, surface pga range) is indicated in each frame.

## COMPARISON WITH EXPERIMENTAL DATA

The analysis performed here on results of numerical simulation has been already performed by Régnier et al. (2016) on instrumental recordings from 174 KiKnet sites. Before proposing the use of the statistical results of numerical simulation in terms of non-linear modulation functions, a prerequisite is to compare them from both qualitative and quantitative viewpoints. In particular, some of the KiKnet soil profiles considered for the numerical simulations correspond to sites which have recorded strong enough motion to allow Régnier et al. (2016) to derive instrumental  $RSR_{NL-L}$  modulation functions. This comparison, still in a preliminary stage, is presented here only along two main items: the general shape of the  $RSR_{NL-L}$  curves, and some statistics on the  $f_{NL}/f_0$  ratio. It may be biased by the fact that only a subset of all KiKnet sites did record very strong motion, nevertheless we consider a statistical comparison on several tens of sites is more meaningful than a comparison on a few sites.

### Qualitative comparison : $RSR_{NL-L}$

First, from a qualitative viewpoint, the overall shapes of both experimental and numerical  $RSR_{NL-L}$  curves are very similar, and their behavior with increasing pga as well :  $f_{NL}$  does not change with pga (except for about 10% of available observations: 3 sites out of a total of 35 exhibit a significant decrease of  $f_{NL}$  from a surface pga of  $1 \text{ m/s}^2$  to  $3 \text{ m/s}^2$ ), while the modulation amplitude increases both at low-frequency ( $f < f_{NL}$ ) and high frequency ( $f > f_{NL}$ ) (see Régnier et al., 2016, for more details).

### Evolution of $f_{NL}/f_0$ as a function of $f_0$

The use of such a "non-linear modulation function" requires the knowledge of the frequency  $f_{NL}$  and of the amplitude modulation. Comparing the numerical and experimental results for the same site classes, i.e. NEHRP B, C and D, indicates a slight underestimation of  $f_{NL}$  values for the former, together with a slight underestimation of the amplitude of the modulation function (smaller increase at low frequency, and smaller decrease at high frequency). The reasons of such differences are not clear yet, and require further investigations, amongst which the test of different NL parameters, especially regarding their depth dependency: there exist indeed consistent indications that the NL parameters used in the present set of numerical simulations underestimate the impact of NL behavior at shallow depth, and overestimate it for thick deposits.

As a support to the latter statement, Figure 10 displays the evolution of the ratio  $f_{NL}/f_0$  as a function of the fundamental frequency  $f_0$  for both the present numerical results and the Régnier et al. (2016) instrumental results. The two plots exhibit the same general trends. First, this ratio is almost systematically exceeding 0.7: the NL behavior never affects thicker soils than those which are involved in the fundamental resonance. Second, the  $f_{NL}/f_0$  may reach values much higher than 1, up to 10 and over: for such sites, the non-linear behavior is mainly affecting much shallower deposits than those involved in the fundamental resonance, especially for thick sites having a low fundamental frequency. There however exist some significant differences between the two plots, i.e., between numerical and instrumental results, especially for low frequency sites : while most of thick sites with  $f_0 < 1 \text{ Hz}$  exhibit an observed  $f_{NL}/f_0$  ratio between 2-3 and about 30, the numerical simulations predict values ranging from 0.7 to 10. This strongly suggests an overestimation of non-linear effects at large depth in the model we used.

The next step is thus to investigate the non-linear response of thick deposits with other sets of degradation curves, exhibiting a more pronounced depth dependence, with larger effects of the confining pressure (i.e. shifting of the degradation curves towards higher strains as the depth increases). Actually, a few tests along this direction were already performed for about 10 thick sites, but the first results do not indicate any major shift of  $f_{NL}$  towards higher values which would correspond to a localization of the non-linear behavior only in the shallow layers. Further tests will be performed in the coming months

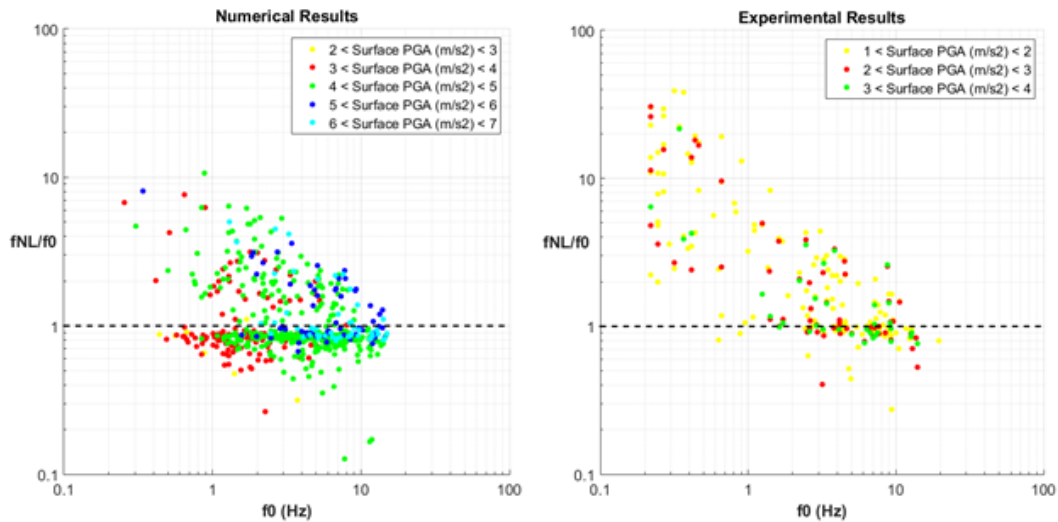


Figure 10. Evolution of  $f_{NL}/f_0$  as a function of  $f_0$  for numerical simulation results (left), and instrumental results (right). The color code corresponds to the surface pga

## CONCLUSIONS

A comprehensive set of numerical simulations has been performed to investigate the non-linear site response for a large number (820) of realistic soil columns covering NEHRP site categories B to E, impinged by a set of 60 realistic strong motion, corresponding to magnitudes between 3 and 7, distances 2 to 100 km, and to outcropping rock pga ranging from 0.02 to 4 m/s<sup>2</sup>. The loading was considered only as vertically incident plane S waves, the soil was assumed dry to avoid the pore pressure effects, and the NL properties were arbitrarily assigned to each soil column as recently done for the NGAW2 background calculations (Kamai et al., 2014). The quantification of the NL response was performed through the "RSR<sub>NL-L</sub>" ratio comparing the NL site response to the linear site response in the Fourier domain, for different ranges of surface pga, in order to allow a direct comparison with the instrumental results obtained by Régner et al. (2016) on a subset of KiKnet data.

Alike the instrumental observations, this RSR<sub>NL-L</sub> "non-linear modulation function" presents almost systematically a typical shape including a low-frequency "over-amplification" and a high-frequency reduction of amplification; the transition between these two behaviors is characterized by a site-specific "non-linear frequency"  $f_{NL}$ .  $f_{NL}$  is found, as in the instrumental observations, to be site-specific, pga independent, systematically larger than  $0.7 f_0$ , and to increase with increasing  $f_0$  and  $V_{S30}$ : in other terms, the stiffer or thinner the surface deposits, the larger the  $f_{NL}$  value. In addition, the  $f_{NL}/f_0$  ratio is found to be around 1 for thin deposits with high fundamental frequency  $f_0$ , and to exhibit a trend to increase and to be much more variable for thicker and/or softer sites. Finally, the amplitude of the modulation (low-frequency increase and high-frequency decrease) is found to increase with increasing surface pga level, with over-amplifications reaching up to 50% in some cases, and reduction levels down to 50%. Average RSR<sub>NL-L</sub> curves are provided for different site classes and different surface pga ranges.

There are however some differences with respect to the instrumental results: the simulated  $f_{NL}$  value has a trend to be smaller and the amount of modulation seems slightly smaller, especially for soft sites. It is likely that such differences are related with the strong assumptions about the NL characteristics of the soil columns, indicating that new series of extensive computations should be performed with other parameterizations, including in particular more non-linearity for shallow, soft soils, and less non-linearity for deep deposits (i.e., with depth larger than 30-50 m), for which the actual effect of confining pressure is not well constrained by actual measurements. Such new simulations should also include other non-linear codes with other constitutive laws (including in the long run effective stress

analysis with pore pressure effects), and probably also a linear equivalent approach, to check the robustness of this RSRNL-L ratio with respect to the NL model.

## ACKNOWLEDGEMENTS

This work benefitted from the support of the SINAPS@ project, a “Seism Institute” project (<http://www.institut-seism.fr/en/>). that receives French funding managed by the National Research Agency under the program “Future Investments” (Sinaps@ reference: ANR-11-RSNR-0022).

## REFERENCES

- Aki, K., and P. Richards, (1980). *Quantitative Seismology. Theory and Methods. W. H. Freeman and Company.*
- Assimaki, D., and W. Li (2012). Site and ground motion-dependent nonlinear effects in seismological model predictions. *Soil Dyn. Earthq. Eng.*, 143 - 151.
- Beresnev, I., and K.L. Wen (1996). Nonlinear soil response, A reality? *Bull. Seism. Soc. Am.* 86 , 1964 - 1978.
- Bonilla, L. (2001). NOAH: User's Manual.
- Bonilla, L.F., K. Tsuda, N. Pulido, J. Regnier, J., and A. Laurendeau (2011). Nonlinear site response evidence of K-net and Kik-net records from the Mw 9 Tohoku earthquake. *Earth Planets Space* 58 , 785-789
- Bonilla, L.-F., R. Archuleta, and D. Lavallée (2005). Hysteretic and dilatant behavior of cohesionless soils and their effects on Nonlinear site response: Field data Observations and modeling. *Bull. Seismol. Soc. Am.* 95 , 2373-2395.
- Cadet, H., P.-Y. Bard, A.-M. Duval, and E. Bertrand (2012). Site effect assessment using Kiknet data: par 2 - site amplification prediction equation based on  $f_0$  and  $V_{sz}$ . *Bull. Earthq. Eng.* 10 , 451 - 489.
- Choi, Y., and J.P. Stewart, 2005. Nonlinear site amplification as function of 30 m shear wave velocity. *Earthq. Spectra* 21, 1–30
- Erdik, M. (1987). Site response analysis. In M. Erdik, & M. Toksöz, Strong ground motion seismology (pp. 479 - 534). Dordrecht: D. Reidel Publishing Company.
- Finn, W. (1991). Geotechnical engineering aspects of microzonation. *Fourth international conference on seismic zonation* Vol. 1, pp. 199 - 2589. Stanford, California.
- Hardin, B., and V. Drnevich, (1972a). Shear modulus and damping in soils: measurement and parameter effects. *J. Soil Mech. Foundations Div. ASCE* 98 , 603 - 624.
- Hardin, B., and V. Drnevich (1972b). Shear modulus and damping in soils: design equations and curves. *J. Soil Mech. Foundations Div. ASCE* 98 , 667 - 692.
- Iai, S., Y. Matsunaga and T. Kameoka (1990). Strain Space Plasticity Model for Cyclic Mobility. *Report of the Port and Harbour Research Institute*, 29, 27 - 56.
- Kamai, R., N.A. Abrahamson and W.J. Silva (2014). Nonlinear horizontal site amplification for constraining the NGA-West 2 GMPEs, *Earthquake Spectra* 30, 1223– 1240
- Kramer, S. (1996). *Geotechnical Earthquake Engineering. Prentice Hall, New Jersey.*
- Régnier, J., H. Cadet, L.F. Bonilla, E. Bertrand and J.-F. Semblat (2013). Assessing nonlinear behavior of soil in seismic site response: Statistical analysis on KiK-net strong motion data. *Bull. Seism. Soc. Am.* 103, 1750 - 1770
- Régnier, J., L.F. Bonilla, E. Bertrand and J.-F. Semblat, (2014). Influence of the  $V_s$  profiles beyond 30 m depth on Linear Site Effects: Assessment from the KiK-net Data. *Bull. Seism. Soc. Am.* 104, 2337 - 2348.
- Régnier, J., H. Cadet and P.-Y. Bard (2016). Empirical quantification of the impact of non-linear soil behavior on site response. *Bull. Seism. Soc. Am.* (accepted, in press)
- Roten, D., Fah, D., & Bonilla, L. (2013). High-frequency ground motion amplification during the 2011 Tohoku earthquake explained by soil dilatancy. *Geophys. J. Int.* 193, 898 - 904.

- Sabetta, F., and A. Pugliese (1996). Estimation of response spectra and simulation of nonstationary earthquake ground motions. *Bull. Seism. Soc. Am.* Vol. 86 (2) , 337 - 352.
- Salameh, C. (2016). Ambient vibrations, spectral contents and seismic damage: a new approach adapted to urban scale. Application to Beirut (Lebanon). *PhD thesis, University Grenoble-Alpes, France*, defended on June 21, 2016 (284 pages, in English)
- Salameh, C., P.-Y. Bard, B. Guillier, J. Harb, C. Cornou and M. Almakari (2016). Using ambient vibration measurements for risk assessment at an urban scale: from numerical proof of concept to a case study in Beirut (Lebanon). Invited keynote lecture, *5<sup>th</sup> IASPEI / IAEE International Symposium: Effects of Surface Geology on Seismic Motion*, Taipei, August 15-17, 2016 (this volume).
- Sandikkaya, M. A., S. Akkar, and P.-Y. Bard, 2013. A nonlinear site-amplification model for the next pan-European ground-motion prediction equations. *Bull. Seism. Soc. Am.*, 103(1), 19-32
- Seed, H., and I. Idriss (1969). Influence of soil conditions on ground motions during earthquakes. *J. Soil Mech. and Foundations. Div. ASCE 95 (SM1)*
- Towhata, I., and K. Ishihara (1985). Modeling Soil Behavior Under Principal axis rotation. *Fifth International Conference on Numerical Methods in Geomechanics*, pp. 523 - 530. Nagoya.
- Walling, M., W. Silva, and N.A. Abrahamson (2008). Nonlinear site amplification factors for constraining the NGA models. *Earthquake Spectra*, 24(1), 243-255